HHS Public Access

Author manuscript

J Biomed Mater Res A. Author manuscript; available in PMC 2020 July 01.

Published in final edited form as:

J Biomed Mater Res A. 2019 July ; 107(7): 1541–1550. doi:10.1002/jbm.a.36668.

Photochemically Crosslinked Cell-laden Methacrylated Collagen Hydrogels with High Cell Viability and Functionality

Thuy-Uyen Nguyen, **Kori E. Watkins**, and **Vipuil Kishore***

Department of Biomedical and Chemical Engineering and Sciences, Florida Institute of Technology, Melbourne, FL 32901

Abstract

Irgacure 2959 (I2959) is widely used as a photoinitiator for photochemical crosslinking of hydrogels. However, the free radicals generated from I2959 have been reported to be highly cytotoxic. In this study, methacrylated collagen (CMA) hydrogels were photochemically crosslinked using two different photoinitiators (i.e., I2959 and VA086) and the effect of photoinitiator type, photoinitiator concentration (i.e., 0.02% and 0.1%) and crosslinking time (1 min and 10 min) on gel morphology, compressive modulus and stability were investigated. In addition, Saos-2 cells were encapsulated within the hydrogels and the effect of photochemical crosslinking conditions on cell viability, metabolic activity and osteoblast functionality was assessed. SEM imaging showed that photochemical crosslinking decreased the porosity of the hydrogels resulting in decrease in water retention ability compared to uncrosslinked hydrogels. On the other hand, photochemical crosslinking improved the stability of CMA hydrogels ($p < 0.05$). Uniaxial compression tests showed that increasing the photoinitiator concentration significantly improved the compressive modulus of CMA hydrogels ($p < 0.05$). Results from the live-dead assay showed that VA086 crosslinked hydrogels exhibited higher cell viability compared to I2959 ($p < 0.05$) crosslinked hydrogels indicating that VA086 is more cytocompatible compared to I2959. Furthermore, Alizarin Red S staining revealed a significantly more pronounced cell-mediated mineralization on VA086 crosslinked hydrogels ($p < 0.05$) indicating that Saos-2 cells retain their normal functionality in the presence of VA086. In summary, these results indicate that VA086 is a more biocompatible photoinitiator compared to I2959 for the generation of photochemically crosslinked CMA hydrogels for tissue engineering applications.

Keywords

methacrylated collagen; photochemical crosslinking; I2959; VA086; Saos-2 cells

1 Introduction

Hydrogels with their superior properties such as biocompatibility, flexibility, and high water content have a wide range of biomedical applications. On a broad scale, depending on the

***Corresponding Author:** Prof. Vipuil Kishore; vkishore@fit.edu; Address: Department of Biomedical and Chemical Engineering and Sciences, Link 319, Florida Institute of Technology, 150 W. University Blvd, Melbourne, FL 32901; Tel: 1-(321)-674-8847; Fax: 1-(321)-674-8437.

type of polymer used, hydrogels can be classified as natural hydrogels (e.g., collagen) or synthetic hydrogels (e.g., poly(ethylene glycol)). Although synthetic hydrogels have certain advantages such as superior mechanical strength, tunable properties, and slow degradation rate, limitations such as poor cell attachment and toxicity of their degradation products limit their widespread use in biomedical applications (1, 2). On the other hand, natural hydrogels are highly biocompatible and contain cell binding sequences (e.g., RGD) that facilitate integrin-mediated cell adhesion and spreading. However, natural hydrogels are mechanically weak and are susceptible to rapid degradation *in vivo*. One approach to address the limitations associated with natural hydrogels is to employ a crosslinking strategy (i.e., physical or chemical) that can help stabilize the polymer network and thereby improve the physical properties of the hydrogel. While chemical crosslinking (e.g., glutaraldehyde, genipin) can significantly improve the mechanical and degradation properties of natural hydrogels, cell encapsulation within the hydrogels can be a concern due to the toxicity of the chemical agents. Therefore, photochemical crosslinking using a photoinitiator and an external light source has gained significant interest for the synthesis of cell-laden hydrogels for tissue engineering applications.

The photopolymerization process is enabled via a photoinitiator which is a light-sensitive reagent that when exposed to a specific light wavelength will dissociate into free radicals that in turn induce the photopolymerization of the hydrogel (3). While many different types of photoinitiators have been investigated (4–8), Irgacure 2959 (I2959) is the most widely used (9–11) due to its high free radical generation efficiency and relatively higher water solubility (3). However, there are concerns related to the cytotoxicity of the free radicals generated using I2959 for fast dividing cell lines (12, 13). Therefore, in search for a more viable photoinitiator, previous studies using alginate and gelatin-based hydrogels have demonstrated that a water soluble azo initiator 2,2’-Azobis[2-methyl-N-(2-hydroxyethyl)propionamide] (VA086) is more cytocompatible and hence can serve as a promising alternative to I2959 for photochemical crosslinking of natural hydrogels (14–19).

Collagen scaffolds are commonly used for tissue engineering applications (20–22) because of their resemblance to the biological properties of most native tissues. While gelatin and collagen have identical amino acid sequences, the secondary structure of these proteins are different and gelatin scaffolds are weaker than collagen scaffolds (23, 24). Further, differences in the stiffness of gelatin and collagen scaffolds have been shown to modulate cellular response (25). Recent work has shown that collagen methacrylation retains the characteristics of native collagen and allows for photochemical crosslinking of collagen-based hydrogels (26). Methacrylated collagen (CMA) has been well characterized and shown to possess 80% free amine groups with a denaturation temperature comparable to native collagen (i.e., 42 °C) (27). While I2959 has been previously used to crosslink CMA (28), to the best of our knowledge, the efficiency of VA086 for photochemical crosslinking of CMA hydrogels and its impact on the physical properties of these hydrogels has not yet been investigated. In addition, the cell-based analyses performed in most existing studies are limited to cell viability and little is known about the impact of VA086 on cell functionality (e.g., ability to generate cell specific *de novo* extracellular matrix).

In this study, we have performed a systematic investigation to optimize the photochemical crosslinking conditions and assess their impact on the physical properties of CMA hydrogels, and osteoblast cell viability and function. Three different photochemical crosslinking parameters were modulated: 1) photoinitiator type (i.e., VA086, I2959), 2) photoinitiator concentration (i.e., 0.1%, 1% w/v), and 3) UV crosslinking time (i.e., 1 min, 10 min). We hypothesized that photochemical crosslinking of CMA hydrogels using VA086 will differentially modulate the physical properties of these hydrogels compared to I2959. Further, we hypothesized that use of VA086 as a photoinitiator will yield higher osteoblast cell viability and better cell functionality. To investigate the impact of different photochemical crosslinking conditions on the physical properties of CMA hydrogels, the following assays were performed: 1) scanning electron microscopy to assess the hydrogel morphology, 2) swelling studies and *in vitro* degradation assays to assess water retention capability and degradation behavior, respectively, 3) uniaxial compression tests to determine compressive modulus. In addition, human osteosarcoma cells (Saos-2) were encapsulated within the hydrogels and the effect of different photochemical crosslinking conditions on cell viability, metabolic activity and functionality was assessed using live/dead cell viability assay, Alamar Blue assay, and Alizarin Red S staining for the detection of cell-mediated mineralization, respectively.

2. Materials and Methods

2.1 Preparation of Photochemically Crosslinked CMA Hydrogels:

Photochemically crosslinked collagen hydrogels were prepared and synthesized from methacrylated collagen type I solution (8 mg/ml; catalog# 5201, Advanced BioMatrix, San Diego, CA) by following the manufacturer's protocol. Briefly, desired volume of photoinitiator (solubilized in methanol) was mixed with neutralized collagen solution and the mixture was added into circular rubber molds (8 mm diameter, 2.5 mm height) and gelled at 37 °C for 30 min. Two types of photoinitiator agents, I2959 (Sigma-Aldrich, MO) and VA086 (Wako, Japan), and two different photoinitiator concentrations (0.02% and 0.1%) were investigated. After gelation, the CMA hydrogels were exposed to a high intensity UV lamp (B-100AP, 365 nm; 15 cm working distance) for two different crosslinking times (i.e., 1 min, 10 min) in order to photochemically crosslink the hydrogels. CMA hydrogels without UV exposure were used as controls.

2.2 Assessment of CMA Morphology using Scanning Electron Microscopy:

The effect of different photochemical crosslinking conditions on the morphology of CMA hydrogels was determined using scanning electron microscopy (SEM). Briefly, the hydrogels were subjected to serial dehydration in ethanol solutions (20%, 50%, 75%, 90%, and 100%), treated with amyl acetate, and subjected to critical-point drying (Denton Vacuum DCP-1 Critical Point Drying Apparatus). The samples were then sputtered with gold and observed at 8000x magnification under SEM (JEOL JSM-6380LV).

2.3 Effect of Photochemical Crosslinking Conditions on Compressive Properties of CMA Hydrogels:

Uniaxial compression tests were performed to determine stiffness of the hydrogels (N = 8/group; DMA Q800, TA Instruments, New Castle, DE). Briefly, CMA hydrogels in a hydrated state (8 mm diameter, 2.5 mm thick) were mounted on the DMA system and a pre-load of 0.0001 N was applied to engage the compression clamp onto the surface of the sample. Following this, the hydrogels were subjected to uniaxial compression at a static loading rate of 0.01 N/min until the compression clamp reached the end position (29). Stress and strain were computed from the load and displacement data. Compressive modulus was determined by taking the slope of the linear region of the stress-strain curve between the 0 and 10% strain (29, 30).

2.4 Effect of Photochemical Crosslinking Conditions on Degradation and Swelling Ratio:

In vitro collagenase degradation assay was performed to determine the stability of the hydrogels (N = 5/group) (31). Briefly, CMA hydrogels were hydrated in ultrapure water for 30 min. Following this, excess water from the hydrogel was removed by gently blotting on a kimwipe and the initial weight (W_0) of the sample was determined. Hydrogels were then incubated in individual micro-centrifuge tubes containing 500 μl of collagenase solution (5 U/ml in 0.1M Tris-HCl buffer and 5mM $CaCl_2$; pH 7.4) at 37 °C. At periodic intervals, the hydrogel was removed from the collagenase solution and weighed (W_t) until the hydrogel was fully degraded. Residual mass was determined by using the following equation:

$$Residual\ Mass(\%) = \frac{w_t}{w_o} \times 100$$

The assess the effect of different photochemical crosslinking conditions on the swelling ratio, CMA hydrogels were lyophilized and weighed to determine the initial dry weight (W_d). Next, the collagen hydrogels were hydrated in 500 μl of 1x PBS for 24 hours and weighed again to determine the wet weight (W_w). The swelling ratio of CMA hydrogels was determined using the equation:

$$Swelling\ Ration(\%) = \frac{W_w - W_d}{W_d} \times 100$$

2.5 Saos-2 Cell Encapsulation within Photochemically Crosslinked CMA Hydrogels:

Human osteosarcoma cell line (Saos-2 cells; HTB-85, ATCC) were expanded in RPMI culture medium supplemented with 15% FBS, 1% L-glutamine, and 1% penicillin/streptomycin. To encapsulate Saos-2 cells (P32) within the CMA hydrogels, cells were first suspended in neutralized CMA solution (with I2959 or VA086 at desired concentrations – 0.02% or 0.1%). Forty five μl of cell suspension was added into each well of a 96-well plate and incubated at 37 °C for 30 min for gelation (5,000 cells/gel). Following this, gels were photocrosslinked by exposing them to UV light (365 nm) for two different times (i.e., 1 min or 10 min). Hydrogels not exposed to UV light were used as controls for cell studies. Cell encapsulated hydrogels were cultured in α-MEM medium supplemented with 50 μg/ml

ascorbic acid, 10 mM β-glycerophosphate, 10% FBS, and 1% penicillin/streptomycin for up to 14 days.

2.6 Effect of Photochemical Crosslinking Conditions on Saos-2 Cell Viability:

Live-dead assay was performed to assess Saos-2 cell viability within CMA hydrogels. After 7 days in culture, collagen hydrogels (N = 3/group) were transferred into a new 24-well plate (Falcon), washed once with 1x PBS and incubated in a solution of 2.5 μM of calcein AM and 2.5 μM ethidium homodimer (Life Technologies) for 15 min at 37 °C. After staining, the gels were imaged under fluorescence microscope (Zeiss) for qualitative assessment of cell viability. For quantification of cell viability, image analyses was performed to determine the percentage of live cells on each hydrogel (N = 6 images/group).

2.7 Effect of Photochemical Crosslinking Conditions on Saos-2 Cell Metabolic Activity:

Alamar blue assay was performed to assess Saos-2 cell metabolic activity (N = 6/group/time point). At periodic intervals (1, 4 and 7 days), cell encapsulated photocrosslinked hydrogels were incubated with 10% Alamar Blue solution (Sigma-Aldrich, MO) for 2 hours at 37 °C. Following this, 100μl of the solution was transferred to another 96 well plate (Greiner) and fluorescence was measured at excitation wavelength of 555 nm and emission wavelength of 595 nm using an M2e Spectramax plate reader (Molecular Devices). Relative fluorescence units (RFU) were used as a measure of cell metabolic activity of Saos-2 cells encapsulated within different CMA hydrogel groups.

2.8 Effect of Photochemical Crosslinking Conditions on Saos-2 Cell-Mediated Mineralization:

Saos-2 cells can serve as a model osteoblast cell line due to their ability to deposit a calcified matrix *in vitro* (32, 33). The effect of different photochemical crosslinking conditions on Saos-2 cell-mediated mineralization was assessed as a measure of *in vitro* cell functionality. After 7 days of culture, 10^{-7} M dexamethasone (Sigma-Aldrich, MO) was added into the culture medium. At day 14, CMA hydrogels were fixed with 10% formaldehyde (Fisher Scientific, USA) for 15 min and washed twice with excess ultra-pure water. Following this, cell-contained CMA hydrogels were stained with 40 mM Alizarin Red S (ARS, pH 4.1; Fisher Scientific, USA) solution for 20 min at room temperature for qualitative assessment of cell-mediated mineralization within the hydrogels. The hydrogels were then washed 5 times with ultra-pure water to remove unbound dye and images of the hydrogels were taken at 1x magnification using a digital camera and at 10x magnification under a microscope (Zeiss). Because ARS is known to bind specifically to calcium, the positive staining (red appearance) is indicative of ongoing Saos-2 cell-mediated mineralization within the CMA hydrogels. To quantify the amount of ARS bound within the CMA hydrogels, 10% acetic acid (Fisher Scientific, USA) solution was added into each hydrogel to extract the ARS stain and the solution pH was adjusted with 10% ammonium hydroxide (Fisher Scientific, USA) until pH ~ 4.1 – 4.5. The solution was then transferred in duplicate into a new 96-well plate (Greiner) and absorbance was read at 405 nm (34).

2.9 Statistical Analyses:

The normality of the data was determined using JMP Pro 14 (JMP Statistical Discovery from SAS, Cary, NC). Normally distributed data were reported as mean + standard deviation and statistical analysis was performed using one-way ANOVA with Tukey post hoc test (JMP). Non-normal data were analyzed using the non-parametric Wilcoxon test and reported as box plots with median, 25th and 75th percentile of data, and whiskers to show the extremes. Statistical significance was set at $p < 0.05$.

3. Results

3.1 Effect of photochemical crosslinking conditions on morphology of photochemically crosslinked methacrylated collagen hydrogels:

SEM analyses revealed that photochemical crosslinking resulted in visible morphological changes within CMA hydrogels (Figure 1). Uncrosslinked hydrogels exhibited a fibrous morphology which is a typical characteristic of collagen hydrogels albeit the fibers appeared to be noticeably thick and densely packed possibly due to the high concentration of collagen in the hydrogels (8 mg/ml; Figure 1A). Upon photochemical crosslinking, either with I2959 or VA086, the fibrous morphology was no longer evident resulting in a scaly appearance and decrease in pore size (Figure 1B-I). Representative images for I2959 (Figure 1B-E) and VA086 (Figure 1F-I) are shown to illustrate that changes in photochemical crosslinking conditions (i.e., photoinitiator type, photoinitiator concentration, crosslinking time) had no impact on the morphology of photochemically crosslinked CMA hydrogels.

3.2 Effect of photochemical crosslinking conditions on compressive modulus of photochemically crosslinked CMA hydrogels:

Uniaxial compression tests showed that the median compressive modulus of uncrosslinked hydrogels was the lowest at around 0.84 (0.78-0.96) kPa (Figure 2). Upon photochemical crosslinking with I2959 at 0.02% concentration, the compressive modulus of the hydrogels was observed to slightly increase but the results were not statistically significant when compared to uncrosslinked hydrogels. However, photochemical crosslinking with VA086 at 0.02% significantly improved the compressive modulus of CMA gels (Figure 2, $p < 0.05$). When photochemical crosslinking was performed using higher concentration of photoinitiator (i.e., 0.1%), a significant increase (> 2-fold; $p < 0.05$) in compressive modulus was observed for both I2959 and VA086 crosslinked hydrogels compared to uncrosslinked hydrogels. In addition, when comparing photoinitiator concentration, the compressive modulus was significantly higher ($p < 0.05$) when using higher concentration of photoinitiator (i.e., 0.1% vs. 0.02%) for both 1 min and 10 min crosslinking times indicating that increasing the concentration of photoinitiator improves the mechanical properties of CMA hydrogels. On the other hand, modulating UV crosslinking time for each photoinitiator concentration had no effect on the compressive modulus of the hydrogel. Lastly, when comparing the two photoinitiators, there was no difference in the compressive modulus of the hydrogels at high concentration of photoinitiator (i.e. 0.1%) though at low concentration (i.e. 0.02%), results showed that the compressive modulus of CMA gels crosslinked with VA086 was 1.5-fold higher ($p < 0.05$) compared to I2959. Together, these

results indicate that photochemical crosslinking helps improve the compressive modulus of CMA hydrogels.

3.3 Effect of photochemical crosslinking conditions on in vitro collagenase degradation and swelling ratio of photochemically crosslinked CMA hydrogels:

In vitro degradation test in collagenase was performed to assess the stability of photochemically crosslinked CMA hydrogels. Results from degradation study showed that uncrosslinked hydrogels degraded rapidly within 4 hours (Figure 3A). However, upon photochemical crosslinking, the degradation time of the hydrogels significantly increased indicating that crosslinking improves the stability of the CMA hydrogels ($p < 0.05$; Figure 3B). Additionally, increasing the photoinitiator concentration and crosslinking time for both photoinitiators further improved the stability of the hydrogels (Figure 3B). When comparing the two photoinitiators at lower concentration (i.e., 0.02%), the rate of degradation was similar. However, at higher photoinitiator concentration (i.e., 0.1%), hydrogels crosslinked with I2959 took significantly longer to degrade compared to VA086 ($p < 0.05$; Figure 3B) suggesting that photochemical crosslinking with I2959 may yield more stable hydrogels. Together, these results indicate photochemical crosslinking is a viable option to generate more stable CMA hydrogels.

Swelling ratio is an important physical property which governs the diffusion of nutrients within the core of the hydrogels and is critical to maintain high cell viability (35, 36). Uncrosslinked CMA hydrogels had a swelling ratio of greater than 90% (Table 1). Expectedly, photochemical crosslinking resulted in a decrease in swelling ratio of the hydrogels. Specifically, photochemical crosslinking with I2959 resulted in a significant decrease in swelling ratio at both 0.02% ($p = 0.0304$) and 0.1% ($p = 0.0163$) photointiator concentration. In addition, CMA hydrogels crosslinked with 0.02% VA086 also showed a significant decrease in swelling ratio ($p = 0.0431$). Photoinitiator type and UV exposure time did not have any effect on the swelling ratio of the CMA hydrogels.

3.4 Effect of photochemical crosslinking conditions on Saos-2 cell viability and metabolic activity:

Cell viability results using live-dead assay showed that cells were more viable in collagen hydrogels photochemically crosslinked with VA086 compared to I2959 (Figure 4A-L). More specifically, cell viability decreased considerably with increase in UV exposure time for I2959 at 0.02% concentration (Figure 4A, 4E, 4I). Further, upon increasing the I2959 concentration to 0.1%, barely any viable cells were observed indicating that higher concentration of I2959 is cytotoxic (Figure 4B, 4F, 4J). On the other hand, increase in UV exposure time triggered no visible change in cell viability for VA086 at 0.02% concentration (Figure 4C, 4G, 4K). Additionally, while the number of viable cells were observed to decrease upon increasing the concentration of VA086 to 0.1% (Figure 4D, 4H, 4L), the number of viable cells were visibly higher on VA086 crosslinked hydrogels compared to those crosslinked with I2959. Quantitative cell viability results obtained via image analyses (i.e., percentage of green vs. red cells) confirmed the visual observations from the fluorescent images (Figure 4M). Increase in UV exposure time from 0 min to 10 min resulted in a significant decrease in cell viability from 75% to 36% ($p = 0.0051$; Figure 4M)

in Saos-2 cells encapsulated within 0.02% I2959 crosslinked collagen hydrogels. Further, cell viability in hydrogels photochemically crosslinked with 0.1% I2959 and exposed to UV for 10 min resulted in a significant drop in cell viability with almost no apparent viable cells ($p = 0.0037$; Figure 4M). On the other hand, modulating the UV exposure time for CMA hydrogels crosslinked with VA086 at high concentration had no impact on cell viability, which was maintained around 75% (Figure 4M). When comparing between the two photoinitiator types, it was evident that cells were more viable in CMA hydrogels crosslinked with VA086, even at higher concentration (0.1%) and longer UV exposure time (10 min), compared to I2959 ($p < 0.05$; Figure 4M). Together, these results indicated that VA086 is more cytocompatible compared to I2959.

Results from Alamar blue assay to assess cell metabolic activity were in agreement with the outcomes observed for cell viability wherein hydrogels with low cell viability also showed low metabolic activity and vice versa (Figure 5). Cells encapsulated within CMA hydrogels without UV exposure continued to proliferate well throughout the 7 day culture period as indicated by the significant increase in RFU values from day 1 to day 4 and day 7 ($p < 0.05$; Figure 5A & 5D). Upon exposure to UV for 1 min, cell metabolic activity significantly increased from day 1 to day 7 for all hydrogels except the ones crosslinked with 0.1% I2959 which showed no change in cell metabolic activity with time (Figure 5B & 5E). When UV exposure time was increased to 10 min, cell metabolic activity was observed to significantly increase from day 1 to day 7 only within CMA hydrogels crosslinked with VA086 and no change in cell metabolic activity was observed in the hydrogels crosslinked with I2959 at both low and high concentration (Figure 5C & 5F). When comparing different UV exposure times, cell metabolic activity decreased with increase in UV exposure time within hydrogels crosslinked with I2959 at both concentrations (Figure 5A-C). On the other hand, cell metabolic activity was observed to be maintained within hydrogels crosslinked with both concentrations of VA086 with 1 min UV exposure time and a slight decrease in cell metabolic activity was observed when UV exposure time was increased to 10 min. Together, these results indicate that Saos-2 cells are able to better retain their cell metabolic activity with VA086 compared to I2959.

3.5 Effect of photochemical crosslinking conditions on Saos-2 cell-mediated mineralization:

Since Saos-2 cells can readily form a mineralized matrix *in vitro*, they can serve as a good model to assess the functionality of cells within biological hydrogels (37). ARS staining was performed to assess Saos-2 cell mediated mineralization within hydrogels photochemically crosslinked with either I2959 or VA086 and 1 min UV crosslinking time. ARS is an anionic dye that stains calcium ions. After 14 days of culture, the results showed some evidence of ARS stained calcium deposits within hydrogels photochemically crosslinked with I2959 (Figure 6A, 6B). For the VA086 crosslinked hydrogels, ARS staining was much richer as evidenced by the dark red coloration which is indicative of more pronounced cell-mediated mineralization (Figure 4C, 4D). Quantitative assessment of ARS staining was performed by extracting the dye and measuring the absorbance at 405 nm. Results showed that the absorbance measurements for dye extracted from hydrogels crosslinked with VA086 was significantly higher compared to I2959 indicating that the extent of Saos-2 cell mediated

mineralization was significantly greater within VA086 crosslinked hydrogels ($p < 0.05$; Figure 6E).

4. Discussion

Cell encapsulation within three-dimensional hydrogels is highly beneficial to recreate the *in vivo* tissue microenvironment. The overarching goal of the current study was to identify the most optimal photochemical crosslinking conditions to generate cell-laden CMA hydrogels and to assess the impact of these parameters on cell viability and function. This is the first study to employ VA086 as a photoinitiator for the crosslinking of CMA hydrogels and the results from this study puts forth a recipe to generate highly biocompatible and functional cell-laden CMA hydrogels that can be used for tissue engineering applications.

Our results on the effect of crosslinking on hydrogel morphology are in agreement with previous work that report that chemical crosslinking triggers collagen fibril merging and thereby result in reduction in pore size (38, 39). However, Gaudet et al. have reported that photochemical crosslinking of CMA hydrogels using I2959 resulted in no change in the morphological appearance of the hydrogel (27). One possible reason for the difference in the outcome may be due to the variation in the concentration of collagen used to synthesize the hydrogels. While Gaudet et al. employed collagen at 3 mg/ml, the current study used a much higher concentration of collagen (8 mg/ml) resulting in a denser network of collagen fibrils and reduced porosity. Further, the collagen fibril diameter within uncrosslinked hydrogels in the current study appeared much thicker compared to the ones synthesized using lower concentration of collagen. Due to these reasons, the collagen fibrils are in much closer proximity to one another and therefore are more likely to coalesce upon crosslinking. CMA hydrogels will need to be synthesized using lower concentrations of collagen to more reliably quantify and compare the effect of different photochemical crosslinking conditions on the pore size distribution within the hydrogels.

The compressive modulus of the collagen hydrogels was determined by taking the steepest slope between the 0% and 10% strain to ensure that the modulus is calculated within the elastic region of the stress-strain curve (29, 40). Results from the current study showed that at high concentration of photoinitiator (0.1%), changing the photoinitiator type (i.e., I2959 vs. VA086) had no effect on the compressive modulus of CMA hydrogels (Figure 2). When assessing the other crosslinking parameters at a fixed light intensity, modulating the photoinitiator concentration as opposed to UV crosslinking time had a more significant impact on the compressive modulus of the hydrogels (Figure 2). Similar outcome was reported in a recent study by O'Connell *et al* that showed that photoinitiator concentration is a critical parameter that governs the rate of the crosslinking reaction (41).

Hydrogel stability is an important factor to determine whether photochemical crosslinking can aid in slowing down the enzymatic degradation of collagen hydrogels once implanted *in vivo* (31, 42). Results from the degradation study are in agreement with a previous study that showed that CMA hydrogels photochemically crosslinked with I2959 degraded significantly slower compared to uncrosslinked hydrogels (27). Specifically, the residual mass of photochemically crosslinked hydrogels was reported to be around 60% at 3 hours which is

comparable to the results observed in the current study (Figure 3A) (27). The decrease in swelling ratio of the CMA hydrogels upon photochemical crosslinking can be attributed to the reduction in pore size (Figure 1) which limits the water retention capability of the hydrogel. Similar outcome has been reported for freeze-dried polyethylene oxide (PEO) hydrogels crosslinked with pentaerythritol tetra-acrylate wherein crosslinking resulted in a noticeable decrease in porosity accompanied by a significant decrease in water retention capability of the PEO hydrogel (86% to 56%) (43). However, it is important to note that the swelling ratio was still greater than 80% after crosslinking suggesting that nutrient transport will not be significantly altered within crosslinked CMA hydrogels.

Previous work has shown that the free radicals generated from I2959 are cytotoxic (3). Results from the current study corroborate with these findings and demonstrate that photoinitiator concentration and UV crosslinking time must be judiciously selected to minimize the toxic effects of I2959. On the contrary, VA086 is highly cytocompatible even when used at significantly higher concentrations than I2959 and UV crosslinking time with VA086 has little effect on cell viability (Figure 4). These results are in agreement with recent studies that compare the effect I2959 and VA086 on cell viability in alginate and methacrylated gelatin hydrogels (14, 15). However, the mechanism due to which I2959 is more cytotoxic compared to VA086 is not well articulated in these studies. One possible reason that may explain the differences between the two photoinitiators in terms of their cytotoxicity may be related to their individual chemical structure. The presence of the hydrophobic acetophenone group in I2959 may enable the photoinitiator to more easily diffuse through the phospholipid bilayer membrane of the cells and thereby induce cell death. Similar outcome has been reported for Irgacure 651 (I651) which is highly hydrophobic (44). On the other hand, the VA086 is more hydrophilic compared to I2959 due to the presence of the aliphatic ketone group and hence may have limited ability to transport through the cell membrane. ARS staining results are in agreement with the cell viability data wherein higher cell-mediated mineralization was observed within hydrogels that contain more viable cells. When comparing the hydrogels crosslinked with different concentrations of VA086, cell-mediated mineralization was observed to be higher on stiffer hydrogels (i.e., 0.1% VA086) compared to softer hydrogels (i.e., 0.02% VA086) as indicated by darker red coloration (Figure 6C, 6D) and an increasing trend in the quantitative data (Figure 6E). These results support the findings reported in the literature that stiffer substrates may be more conducive to bone differentiation (45). Together, these results indicate that photochemical crosslinking with VA086 maintains Saos-2 cell functionality within CMA hydrogels.

Overall, the results from the current study demonstrate that photochemical crosslinking induces morphological changes within CMA hydrogels characterized by fibril merging and reduction in porosity. The compressive modulus of the CMA hydrogels photochemically crosslinked with high concentrations of I2959 or VA086 was comparable. However, cell viability, metabolic activity and functionality were better preserved in CMA hydrogels photochemically crosslinked with VA086 compared to I2959. Although short-term culture (i.e., 7 days) using Saos-2 cells is a good model to assess the biocompatibility of collagen-based hydrogels (32, 46), future studies will build upon this work and assess tissue-specific cellular differentiation of human mesenchymal stem cells using longer-term cultures (i.e., up

to 4 weeks). CMA hydrogel in combination with I2959 has been used as bio-ink for 3D bioprinting applications (28). Based on the outcomes of the current study, we suggest that VA086 can serve as an effective replacement for I2959 for the synthesis of cell-laden CMA hydrogels and in the development of viable bio-inks for 3D printing of collagen-based biomimetic scaffolds for tissue engineering applications.

Acknowledgments:

This study was supported by the National Institute of Arthritis and Musculoskeletal and Skin Diseases of the National Institute of Health (NIH 1R15AR071102). The content reported here is solely the responsibility of the authors and does not necessarily represent the official views of the NIH.

References

1. Drury JL, Mooney DJ. Hydrogels for tissue engineering: scaffold design variables and applications. Biomaterials 2003;24:4337–4351. [PubMed: 12922147]
2. Lee JH, Kim HW. Emerging properties of hydrogels in tissue engineering. J Tissue Eng 2018;9:2041731418768285. [PubMed: 29623184]
3. Williams CG, Malik AN, Kim TK, Manson PN, Elisseeff JH. Variable cytocompatibility of six cell lines with photoinitiators used for polymerizing hydrogels and cell encapsulation. Biomaterials 2005;26:1211–1218. [PubMed: 15475050]
4. Rich H, Odlyha M, Cheema U, Mudera V, Bozec L. Effects of photochemical riboflavin-mediated crosslinks on the physical properties of collagen constructs and fibrils. J Mater Sci Mater Med 2014;25:11–21. [PubMed: 24006048]
5. Arakawa C, Ng R, Tan S, Kim S, Wu B, Lee M. Photopolymerizable chitosan-collagen hydrogels for bone tissue engineering. J Tissue Eng Regen Med 2017;11:164–174. [PubMed: 24771649]
6. Madden LR, Mortisen DJ, Sussman EM, Dupras SK, Fugate JA, Cuy JL, Hauch KD, Laflamme MA, Murry CE, Ratner BD. Proangiogenic scaffolds as functional templates for cardiac tissue engineering. Proc Natl Acad Sci USA 2010;107:15211–15216. [PubMed: 20696917]
7. Bryant S, Nuttelman C, Anseth K. Cytocompatibility of UV and visible light photoinitiating system on cultured NIH/3T3 fibroblasts. J Biomater Sci Polym Ed 2000;11:439–457. [PubMed: 10896041]
8. Hwang J, Noh S, Kim B, Jung H. Gelation and crosslinking characteristics of photopolymerized poly(ethylene glycol) hydrogels. J Appl Polym Sci 2015;132:41939.
9. Chou AI, Nicoll SB. Characterization of photocrosslinked alginate hydrogels for nucleus pulposus cell encapsulation. J Biomed Mater Res A 2009;91:187–194. [PubMed: 18785646]
10. Stratesteffen H, Kopf M, Kreimendahl F, Blaeser A, Jockenhoevel S, Fischer H. GelMA-collagen blends enable drop-on-demand 3D printablility and promote angiogenesis. Biofabrication 2017;9:045002-5090/aa857c.
11. Sawyer SW, Shridhar SV, Zhang K, Albrecht LD, Filip AB, Horton JA, Soman P Perfusion directed 3D mineral formation within cell-laden hydrogels. Biofabrication 2018;10:035013-5090/aacb42.
12. Harris S, Enger R, Riggs B, Spelsberg T. Development and characterization of a conditionally immortalized human fetal osteoblastic cell line. J Bone Miner Res 1995;10:178–186. [PubMed: 7754797]
13. Shamblott MJ, Axelman J, Wang S, Bugg EM, Littlefield JW, Donovan PJ, Blumenthal PD, Huggins GR, Gearhart JD. Derivation of pluripotent stem cells from cultured human primordial germ cells. Proc Natl Acad Sci USA 1998;95:13726–13731. [PubMed: 9811868]
14. Rouillard AD, Berglund CM, Lee JY, Polacheck WJ, Tsui Y, Bonassar LJ, Kirby BJ. Methods for photocrosslinking alginate hydrogel scaffolds with high cell viability. Tissue Eng Part C Methods 2011;17:173–179. [PubMed: 20704471]
15. Billiet T, Gevaert E, De Schryver T, Cornelissen M, Dubruel P. The 3D printing of gelatin methacrylamide cell-laden tissue-engineered constructs with high cell viability. Biomaterials 2014;35:49–62. [PubMed: 24112804]

16. Chandler EM, Berglund CM, Lee JS, Polacheck WJ, Gleghorn JP, Kirby BJ, Fischbach C. Stiffness of photocrosslinked RGD-alginate gels regulates adipose progenitor cell behavior. Biotechnol Bioeng 2011;108:1683–1692. [PubMed: 21328324]
17. Coates EE, Riggin CN, Fisher JP. Photocrosslinked alginate with hyaluronic acid hydrogels as vehicles for mesenchymal stem cell encapsulation and chondrogenesis. J Biomed Mater Res A 2013;101:1962–1970. [PubMed: 23225791]
18. Occhetta P, Visone R, Russo L, Cipolla L, Moretti, M, Rasponi M. VA-086 methacrylate gelatine photopolymerizable hydrogels: A parametric study for highly biocompatible 3D cell embedding. J Biomed Mater Res A 2015;103:2109–2117. [PubMed: 25294368]
19. Lin CH, Lin KF, Mar K, Lee SY, Lin YM. Antioxidant N-Acetylcysteine and Glutathione Increase the Viability and Proliferation of MG63 Cells Encapsulated in the Gelatin Methacrylate/VA-086/Blue Light Hydrogel System. Tissue Eng Part C Methods 2016;22:792–800. [PubMed: 27406060]
20. Keogh MB, O'Brien FJ, Daly JS. A novel collagen scaffold supports human osteogenesis--applications for bone tissue engineering. Cell Tissue Res 2010;340:169–177. [PubMed: 20198386]
21. Lu D, Mahmood A, Qu C, Hong X, Kaplan D, Chopp M. Collagen scaffolds populated with human marrow stromal cells reduce lesion volume and improve functional outcome after traumatic brain injury. Neurosurgery 2007;61:596–602; discussion 602–3. [PubMed: 17881974]
22. Davidenko N, Campbell JJ, Thian ES, Watson CJ, Cameron RE. Collagen-hyaluronic acid scaffolds for adipose tissue engineering. Acta Biomater 2010;6:3957–3968. [PubMed: 20466086]
23. Zeugolis DI, Khew ST, Yew ES, Ekaputra AK, Tong YW, Yung LL, Hutmacher DW, Sheppard C, Raghunath M. Electro-spinning of pure collagen nano-fibres–just an expensive way to make gelatin? Biomaterials 2008;29:2293–2305. [PubMed: 18313748]
24. Ratanavaraporn J, Damrongsakkul S, Sanchavanakit N, Banaprasert T, Kanokpanont S. Comparison of gelatin and collagen scaffolds for fibroblast cell culture. Journal of Metals, Materials and Minerals 2006;16:31–36.
25. Tsai SW, Liou HM, Lin CJ, Kuo KL, Hung YS, Weng RC, Hsu FY. MG63 osteoblast-like cells exhibit different behavior when grown on electrospun collagen matrix versus electrospun gelatin matrix. PLoS One 2012;7:e31200. [PubMed: 22319618]
26. Drzewiecki KE, Parmar AS, Gaudet ID, Branch JR, Pike DH, Nanda V, Shreiber DI. Methacrylation induces rapid, temperature-dependent, reversible self-assembly of type-I collagen. Langmuir 2014;30:11204–11211. [PubMed: 25208340]
27. Gaudet ID, Shreiber DI. Characterization of methacrylated type-I collagen as a dynamic, photoactive hydrogel. Biointerphases 2012;7:25-012-0025-y Epub 2012 Mar 10.
28. Drzewiecki KE, Malavade JN, Ahmed I, Lowe CJ, Shreiber DI. A thermoreversible, photocrosslinkable collagen bio-ink for free-form fabrication of scaffolds for regenerative medicine. Technology (Singap World Sci) 2017;5:185–195. [PubMed: 29541655]
29. Worthington KS, Wiley LA, Bartlett AM, Stone EM, Mullins RF, Salem AK, Guymon CA, Tucker BA. Mechanical properties of murine and porcine ocular tissues in compression. Exp Eye Res 2014;121:194–199. [PubMed: 24613781]
30. Borges A, Bourban P, Pioletti D, Manson J. Curing kinetics and mechanical properties of composite hydrogel for the replacement of the nucleus pulposus. Compos. Sci. Technol 2010;70:1847–1853.
31. Ahn JI, Kuffova L, Merrett K, Mitra D, Forrester JV, Li F, Griffith M. Crosslinked collagen hydrogels as corneal implants: effects of sterically bulky vs. non-bulky carbodiimides as crosslinkers. Acta Biomater 2013;9:7796–7805. [PubMed: 23619290]
32. Liu G, Pastakia M, Fenn MB, Kishore V. Saos-2 cell-mediated mineralization on collagen gels: Effect of densification and bioglass incorporation. J Biomed Mater Res A 2016;104:1121–1134. [PubMed: 26750473]
33. Nijsure MP, Pastakia M, Spano J, Fenn MB, Kishore V. Bioglass incorporation improves mechanical properties and enhances cell-mediated mineralization on electrochemically aligned collagen threads. Journal of Biomedical Materials Research Part A 2017.
34. Kerativitayanan P, Tatullo M, Khariton M, Joshi P, Perniconi B, Gaharwar AK. Nanoengineered Osteoinductive and Elastomeric Scaffolds for Bone Tissue Engineering. ACS Biomater Sci Eng 2017;3:590–600.

35. Nazemi K, Moztarzadeh F, Jalali N, Asgari S, Mozafari M. Synthesis and characterization of poly(lactic-co-glycolic) acid nanoparticles-loaded chitosan/bioactive glass scaffolds as a localized delivery system in the bone defects. Biomed Res Int 2014;2014:898930. [PubMed: 24949477]

36. Bryant SJ, Anseth KS, Lee DA, Bader DL. Crosslinking density influences the morphology of chondrocytes photoencapsulated in PEG hydrogels during the application of compressive strain. J Orthop Res 2004;22:1143–1149. [PubMed: 15304291]

37. Czekanska EM, Stoddart MJ, Richards RG, Hayes JS. In search of an osteoblast cell model for in vitro research. Eur Cell Mater 2012;24:1–17. [PubMed: 22777949]

38. Natarajan V, Krithica N, Madhan B, Sehgal PK. Preparation and properties of tannic acid cross-linked collagen scaffold and its application in wound healing. J Biomed Mater Res B Appl Biomater 2013;101:560–567. [PubMed: 23255343]

39. Bridgeman CJ, Nguyen TU, Kishore V. Anticancer efficacy of tannic acid is dependent on the stiffness of the underlying matrix. J Biomater Sci Polym Ed 2018;29:412–427. [PubMed: 29285987]

40. Mouser VH, Melchels FP, Visser J, Dhert WJ, Gawlitta D, Malda J. Yield stress determines bioprintability of hydrogels based on gelatin-methacryloyl and gellan gum for cartilage bioprinting. Biofabrication 2016;8:035003–5090/8/3/035003. [PubMed: 27431733]

41. O'Connell CD, Zhang B, Onofrillo C, Duchi S, Blanchard R, Quigley A, Bourke J, Gambhir S, Kapsa R, Di Bella C, Choong P, Wallace GG. Tailoring the mechanical properties of gelatin methacryloyl hydrogels through manipulation of the photocrosslinking conditions. Soft Matter 2018;14:2142–2151. [PubMed: 29488996]

42. Ravichandran R, Islam MM, Alarcon EI, Samanta A, Wang S, Lundstrom P, Hilborn J, Griffith M, Phopase J. Functionalised type-I collagen as a hydrogel building block for bio-orthogonal tissue engineering applications. Journal of Materials Chemistry B 2016;4:318–326.

43. Wong RS, Ashton M, Dodou K. Effect of Crosslinking Agent Concentration on the Properties of Unmedicated Hydrogels. Pharmaceutics 2015;7:305–319. [PubMed: 26371031]

44. Mironi-Harpaz I, Wang DY, Venkatraman S, Seliktar D. Photopolymerization of cell-encapsulating hydrogels: crosslinking efficiency versus cytotoxicity. Acta Biomater 2012;8:1838–1848. [PubMed: 22285429]

45. Engler AJ, Sen S, Sweeney HL, Discher DE. Matrix elasticity directs stem cell lineage specification. Cell 2006;126:677–689. [PubMed: 16923388]

46. Rothamel D, Schwarz F, Sculean A, Herten M, Scherbaum W, Becker J. Biocompatibility of various collagen membranes in cultures of human PDL fibroblasts and human osteoblast-like cells. Clin Oral Implants Res 2004;15:443–449. [PubMed: 15248879]

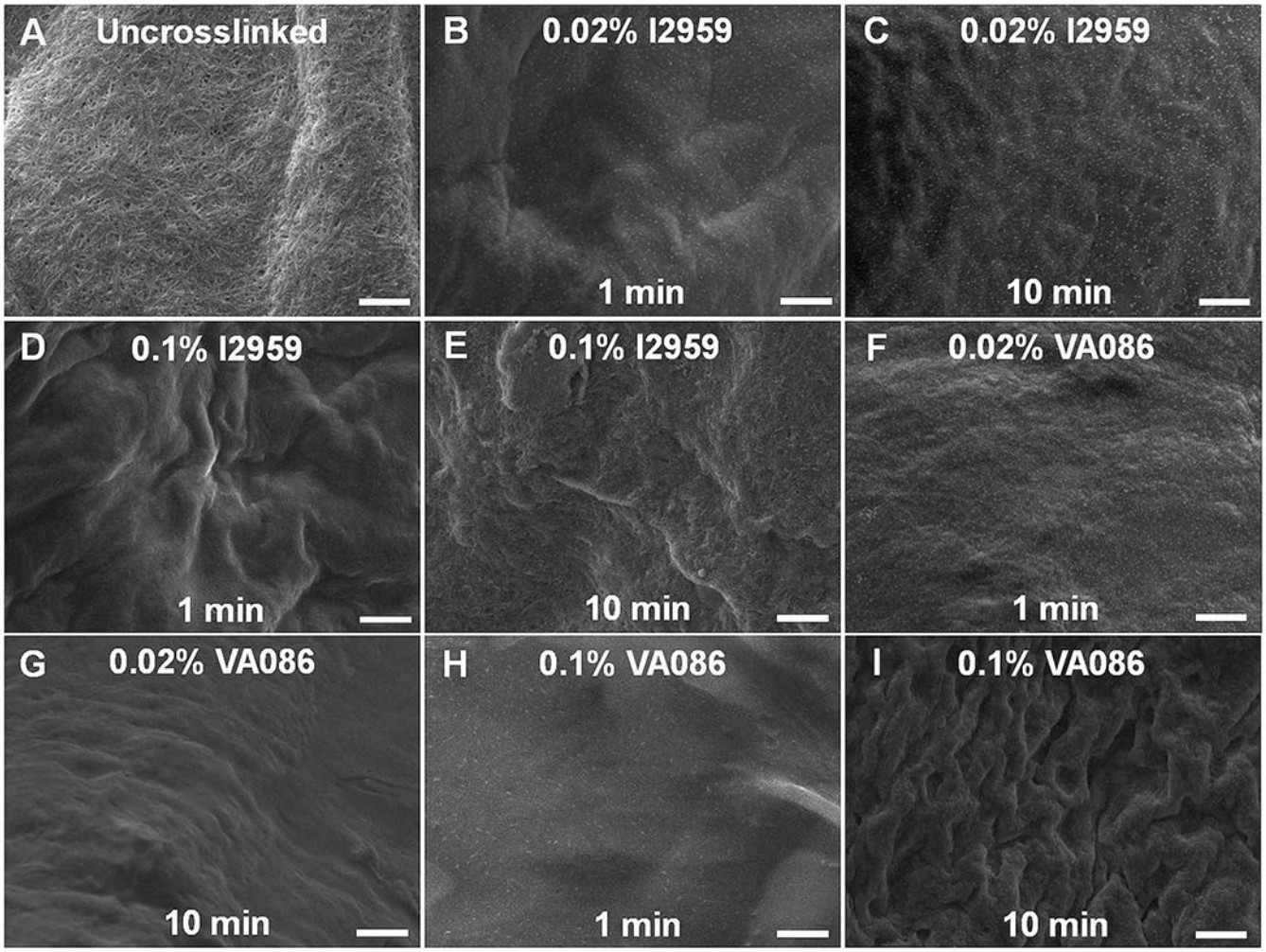

Figure 1:

Assessment of photochemically crosslinked CMA hydrogel morphology via SEM. (A) Uncrosslinked CMA hydrogel, (B-E) CMA hydrogels photochemically crosslinked with I2959 and (F-I) CMA hydrogels photochemically crosslinked with VA086. Scale bar: 2 μm.

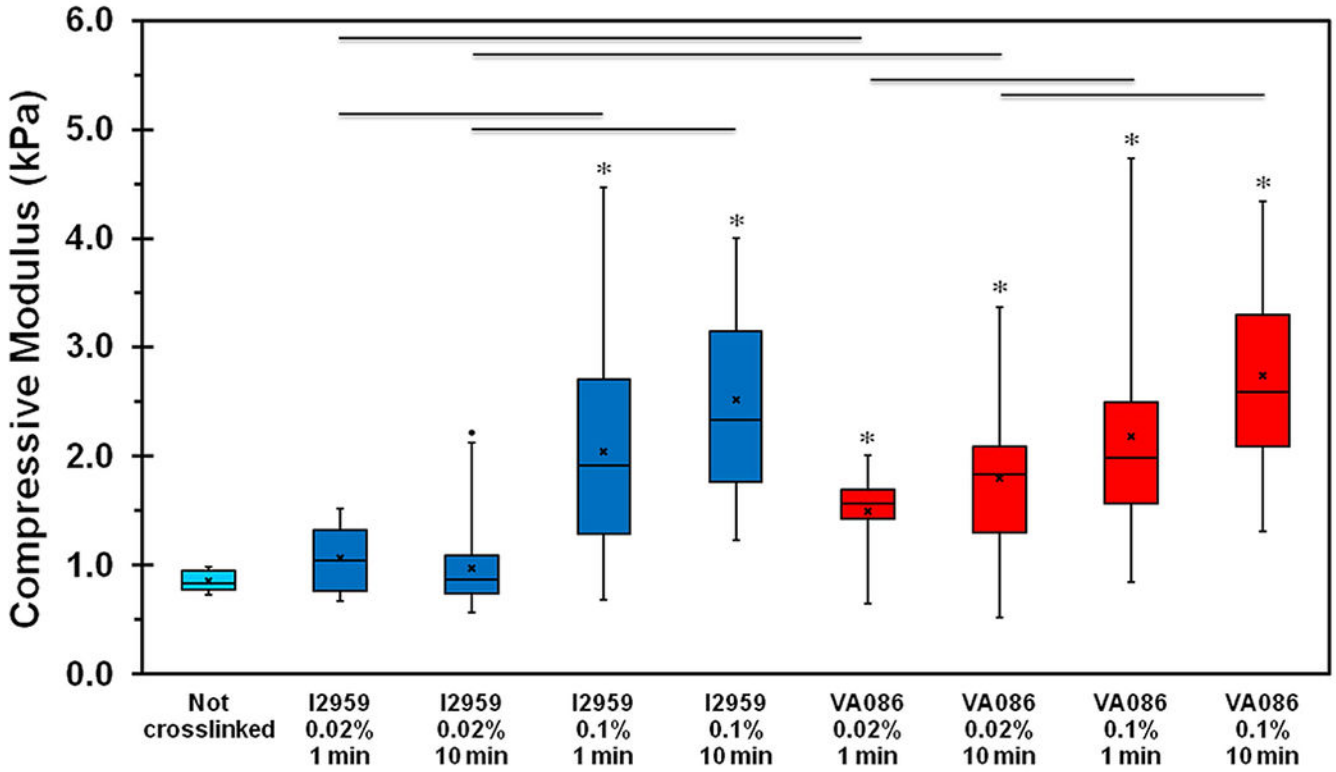

Figure 2:

Mechanical assessment of photochemically crosslinked CMA hydrogels. Compressive modulus determined at 10% strain region. The boxes represent 25th to 75th percentile of the data separated by a horizontal line at the median. The whiskers show the upper and lower extremes. “x” mark shows the mean and dot shows the outlier (‘*’ denotes $p < 0.05$ between crosslinked hydrogels and uncrosslinked hydrogels; horizontal lines denote $p < 0.05$ between connecting groups).

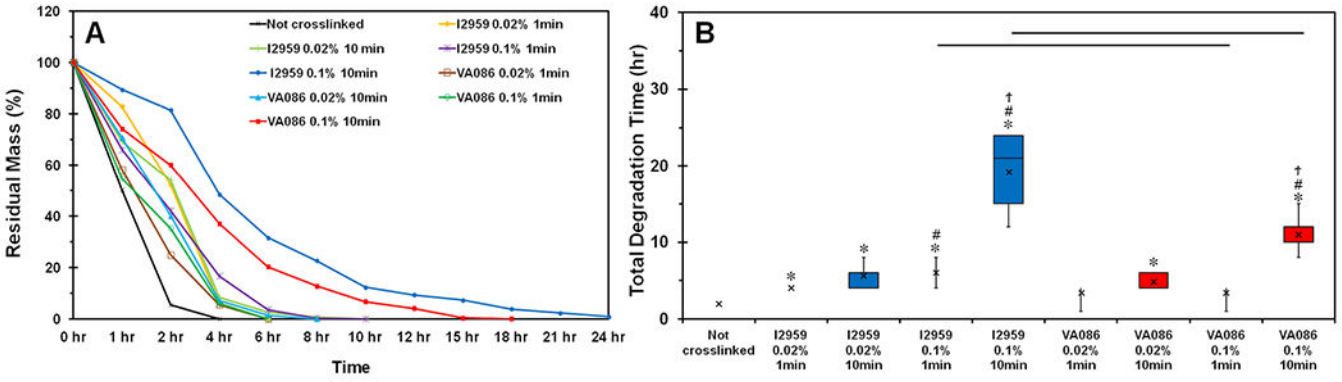

Figure 3:

In vitro collagenase degradation of photochemically crosslinked CMA hydrogels. The boxes represent 25th to 75th percentile of the data separated by a horizontal line at the median. The whiskers show the upper and lower extremes. "x" mark shows the mean (**'*'** denotes $p < 0.05$ when compared to not crosslinked hydrogels; **'#'** denotes $p < 0.05$ when comparing 0.02% and 0.1% photoinitiator concentration for the same photoinitiator type and crosslinking time; **'†'** denotes $p < 0.05$ when comparing between 1 min and 10 min groups of the same photoinitiator type and concentration; horizontal lines denote $p < 0.05$ between photoinitiator type).

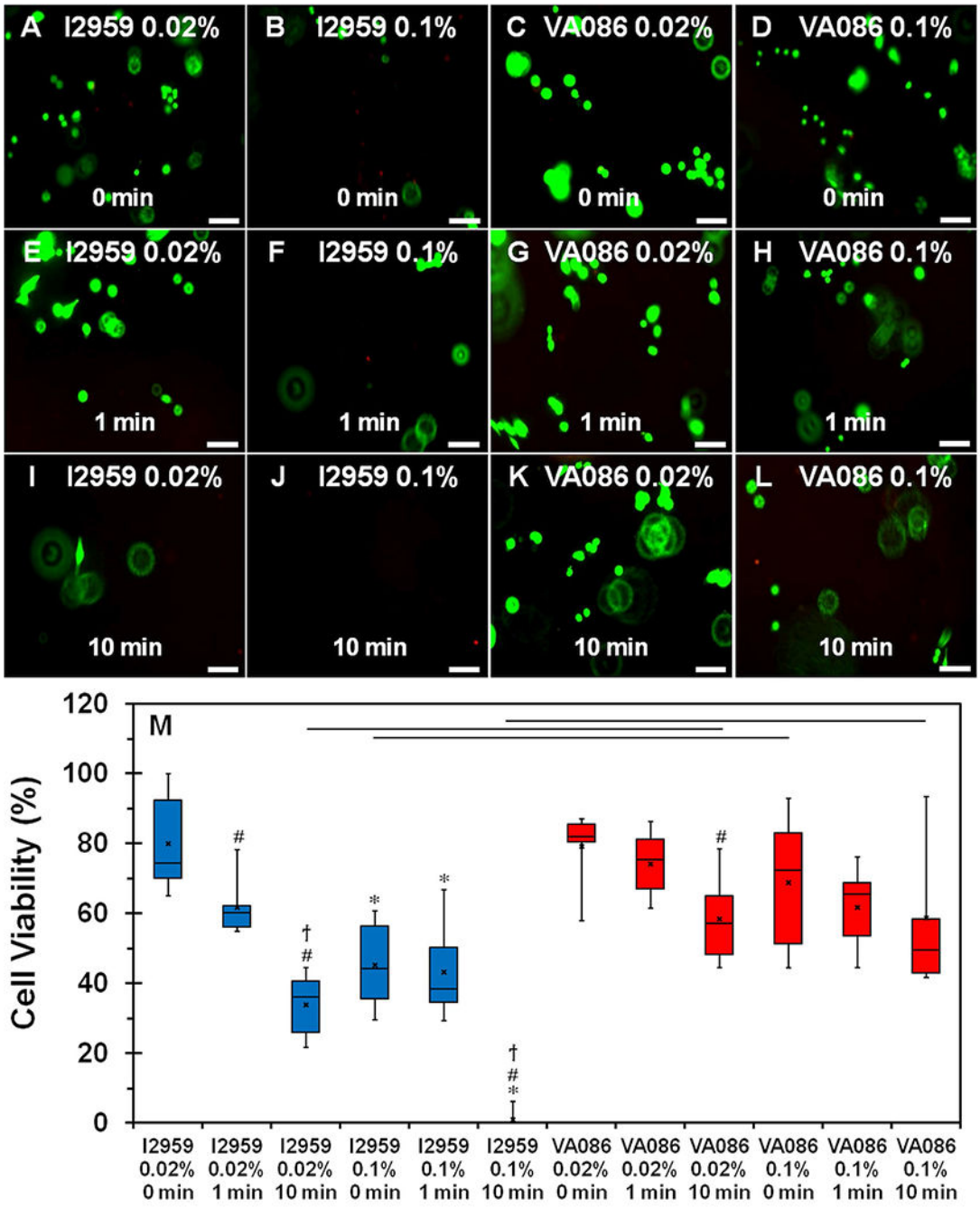

Figure 4:

(A-L) Live-dead assay to assess the viability of Saos-2 cells cultured within photochemically crosslinked CMA hydrogels (live cells stain green and dead cells stain red). (M) Quantification of cell viability plot. The boxes represent 25th to 75th percentile of the data separated by a horizontal line at the median. The whiskers show the upper and lower extremes. "x" mark shows the mean (**'*'** denotes $p < 0.05$ when comparing different photoinitiator concentration for the same photoinitiator type and crosslinking time, **'#'** denotes $p < 0.05$ when comparing 1 min and 10 min crosslinking times with 0 min for the

same photoinitiator type and concentration; **‘†’** denotes $p < 0.05$ when comparing between 1 min and 10 min crosslinking times for the same photoinitiator type and concentration; horizontal line denotes $p < 0.05$ between photoinitiator type). Scale bar: 100 μm.

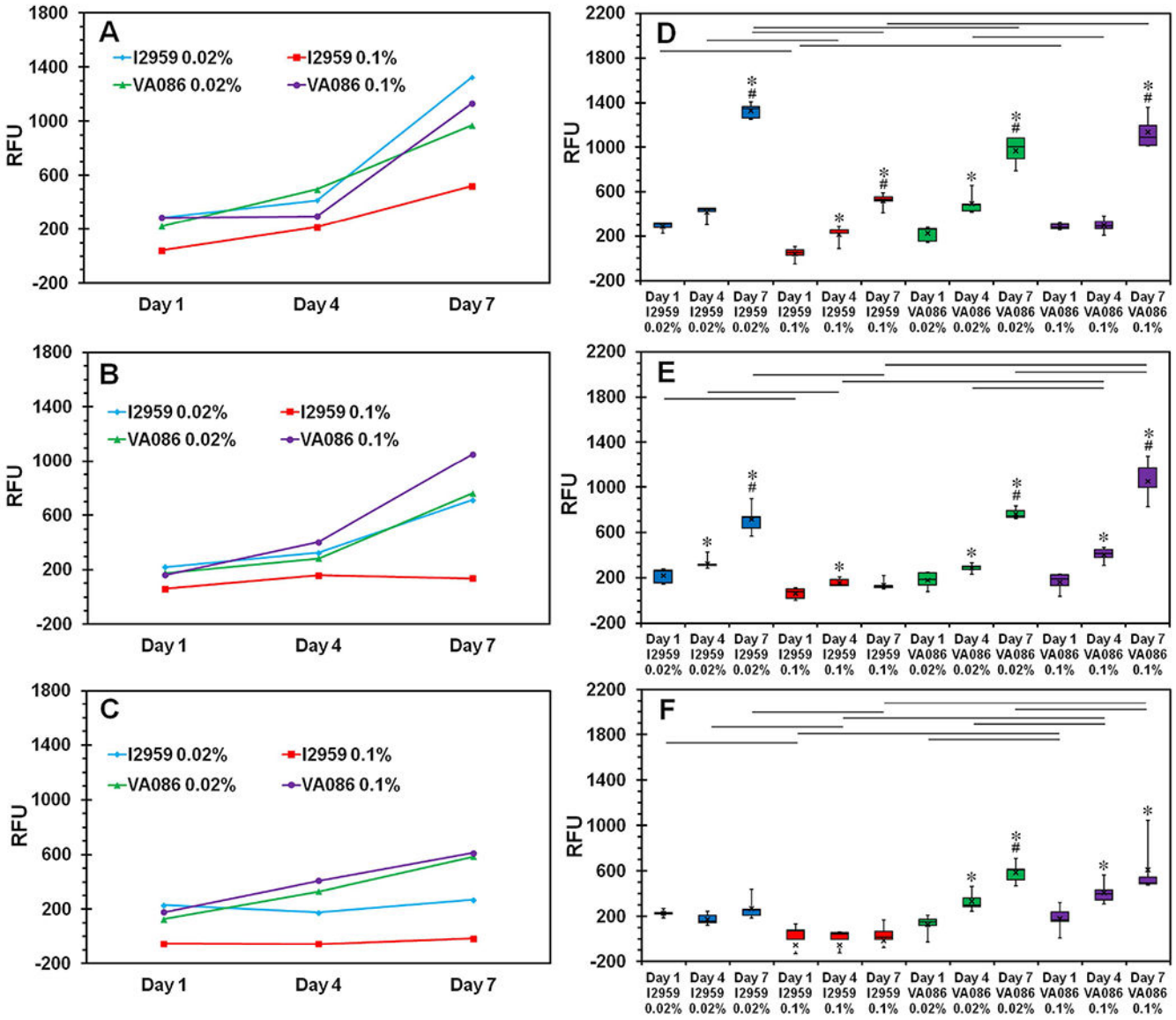

Figure 5:

Quantification of cell metabolic activity on photochemically crosslinked CMA hydrogels using Alamar blue assay. (A-C) Line plots show the average relative fluorescence units (RFU) as a measure of cell metabolic activity trend from day 1 to day 7. (D-F) Whisker and box plots for statistical comparison of different photochemical crosslinking conditions on cell metabolic activity - (A, D) 0 min, (B, E) 1 min, and (C, F) 10 min. The boxes represent 25^{th} to 75^{th} percentile of the data separated by a horizontal line at the median. The whiskers show the upper and lower extremes. "x" mark shows the mean (**'*'** denotes $p < 0.05$ when comparing day 7 and day 4 with day 1 for the same photoinitiator type and concentration; **'#'** denotes $p < 0.05$ when comparing day 7 with day 4 for the same photoinitiator type and concentration; **horizontal lines** denote $p < 0.05$ between connecting groups at the same culture time point).

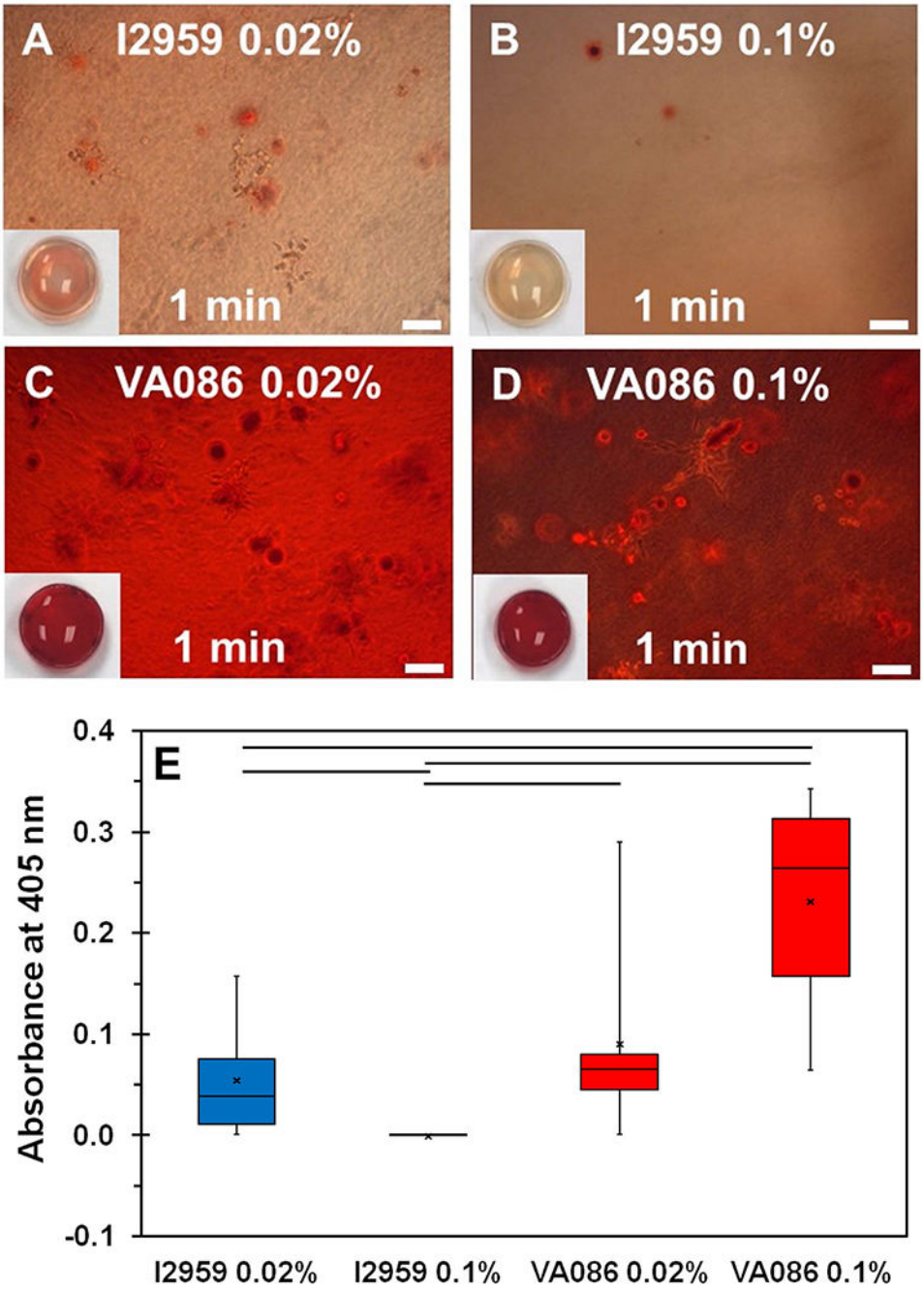

Figure 6:

(A-D) Qualitative assessment of Saos-2 cell-mediated mineralization within photochemically crosslinked CMA hydrogels via ARS staining. Scale bar: 100 μm. Insets show 1x magnification images of the actual ARS stained hydrogels (6 mm diameter). (E) Quantification of ARS staining. The boxes represent 25th to 75th percentile of the data separated by a horizontal line at the median. The whiskers show the upper and lower

extremes. “x” mark shows the mean (horizontal line denotes $p < 0.05$ when comparing between photoinitiator type).

Table 1:

Swelling ratio for photochemically crosslinked CMA hydrogels.

Hydrogel	Swelling Ratio (%)
Not Crosslinked	91.9 ± 1.4
I2959 0.02% 1 min	82.6 ± 5.5 *
I2959 0.02% 10 min	80.5 ± 4.8 *
I2959 0.1% 1 min	81.9 ± 5.0 *
I2959 0.1% 10 min	84.2 ± 3.3
VA086 0.02% 1 min	87.2 ± 2.0
VA086 0.02% 10 min	82.9 ± 6.3 *
VA086 0.1% 1 min	88.6 ± 3.6
VA086 0.1% 10 min	84.8 ± 3.6

* denotes $p < 0.05$ when comparing crosslinked hydrogels with not crosslinked hydrogels